MACROPHAGE ACTIVATION IN SICKLE CELL DISEASE: THE ROLE OF SPHINGOLIPID METABOLISM IN THE DISEASE STATE

A Thesis
Presented to
The Academic Faculty

by

Alicia Lane

In Partial Fulfillment
of the Requirements for the Degree
Bachelor of Science in the
School of Biology

Georgia Institute of Technology
May 2015

MACROPHAGE ACTIVATION IN SICKLE CELL DISEASE: THE ROLE OF SPHINGOLIPID METABOLISM IN THE DISEASE STATE

This document contains unpublished results. Please do not disseminate or publish this information.

Approved by:

Dr. Edward Botchwey, Advisor
School of Biomedical Engineering
Georgia Institute of Technology

Dr. Greg Gibson
School of Biology
Georgia Institute of Technology

Date Approved: April 11, 2014

ACKNOWLEDGEMENTS

I would like to express my gratitude to the Petit Scholars Program for introducing me to research. Special thanks go to Tony Awojoodu and Ed Botchwey for their help and support throughout my time in the lab, for trusting me to do my own projects, encouraging me to think big, and helping me discover my passion for research. I would also like to thank Phil Keegan and the Platt Lab for their assistance in the lab and Greg Gibson for his advice and comments as I worked on my thesis. Finally, I would like to thank my family and friends for keeping me grounded and encouraging me to pursue what I love.

TABLE OF CONTENTS

LIST OF FIGURES

Page

NOMENCLATURE

SCD	Sickle cell disease
SS	Two mutated alleles (has SCD)
AA	Two normal alleles (does not have SCD)
S1P	Sphingosine-1-phosphate
Sph	Sphingosine
MP	Microparticle
M0	M0 macrophage
M1	M1 macrophage (inflammatory, classically-activated)
M2	M2 macrophage (anti-inflammatory, alternatively-activated)
RBC	Red blood cell
PBMC	Peripheral blood mononuclear cell

SUMMARY

Sickle cell disease (SCD) is a disorder in which defective hemoglobin causes sickling of red blood cells, inducing painful vaso-occlusive crises when blood flow is blocked at sites of red blood cell (RBC) clotting that can ultimately result in organ failure or death. This work demonstrates that sphingolipid metabolism is dysregulated in SCD and that this pathway can be targeted pharmacologically to prevent vaso-occlusion. We suggest a pathway in which the sickling of RBCs in SCD activates acid sphingomyelinase, altering the distribution and concentration of sphingolipids in the RBC membrane and resulting in the production of sphingolipid-rich microparticles that are secreted and can interact with cells in circulation. Sphingosine-1-phosphate (S1P) is believed to be a key modulator of SCD because it is stored at high concentrations in RBCs. Sphingolipid metabolism was confirmed to be dysregulated in SCD; most notably, S1P was significantly elevated in RBCs, and plasma, and microparticles, and the activity of acid sphingomyelinase and concentration of its byproduct, microparticles, were significantly elevated in SCD RBCs. Treatment of monocytes with S1P and SCD RBCs increased their adhesion over four-fold to endothelial cells, indicating that altered sphingolipid distribution in RBCs may contribute to vaso-occlusion through increasing myeloid cell adhesion. A cytokine profile of macrophages treated with SCD microparticles suggest that microparticles play a role in this process by increasing the secretion of inflammatory cytokines associated with SCD crises, including MIP-1α, IL-6, and TNF-α. Pilot *in vitro* studies in RBCs and *in vivo* studies in mice implicate that drugs targeting the sphingolipid metabolic pathway may be more effective treatment options than blood transfusions in managing SCD and preventing vaso-occlusive crises.

CHAPTER 1

INTRODUCTION

Sickle cell disease (SCD) is a blood disorder caused by a point mutation in the gene for hemoglobin (Embury, 1986). Defective hemoglobin results in sickling of red blood cells (RBCs) and increased clotting (Belcher et al., 2000; Kaul et al., 2009). As shown in Figure 1, macrophages and monocytes, myeloid-derived immune cells, are activated in the disease state and adhere at these clots, further contributing to inflammation and vaso-occlusion (Belcher et al., 2000), which in extreme cases can ultimately result in organ failure and death (Madigan and Malik, 2006). The estimated number of people with SCD in the United States is between 70,000 and 100,000, and in African Americans the disease is observed in 1 out of every 500 births (National Institutes of Health, 2012). Currently, SCD treatment entails pain management and blood transfusions to replace sickled RBCs, but these methods are not always effective and can result in treatment-related complications over time (Harmatz et al., 2000).

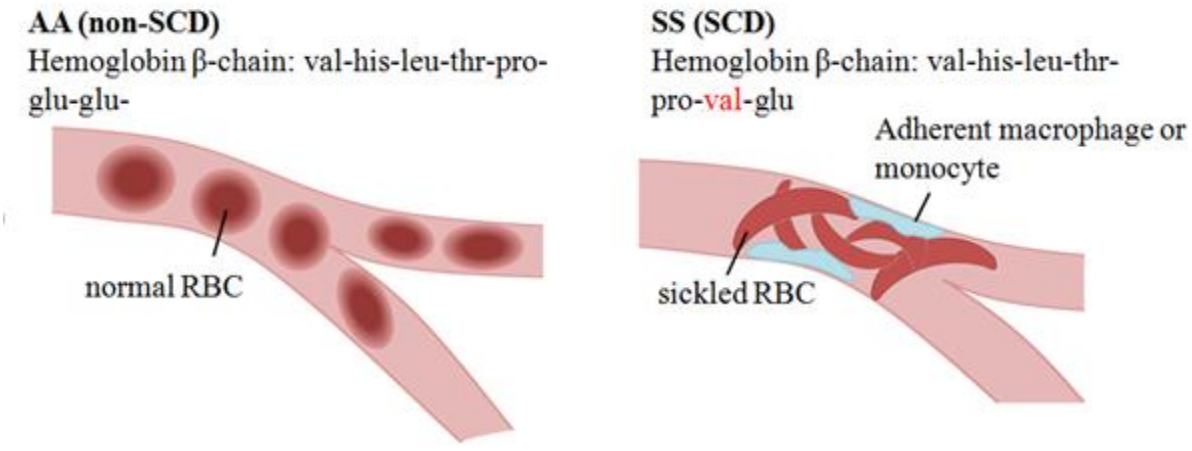

Figure 1. Schematic of healthy red blood cell function versus clotting and myeloid cell adhesion in SCD. (A) Healthy RBCs can pass easily through blood vessels. (B) Sickled red blood cells are less flexible and tend to create clots. Myeloid cells like macrophages and monocytes can become activated and adhere at these sites, further blocking blood flow.

This work investigates dysregulated sphingolipid metabolism as an underlying cause of the pathology of SCD and demonstrates that this pathway is open to pharmacological therapies that can be used to treat the disease (Figure 2). Sphingolipids are a family of lipids that play a key role in cell membrane dynamics and signaling (van Meer et al., 2008). Sphingosine 1-phosphate (S1P) is an immunomodulatory sphingolipid that is of special interest for SCD because it is highly concentrated in red blood cells (Peest et al., 2008) and is elevated in SCD (Awojoodu, unpublished). The Botchwey lab believes that membrane stress induced by RBC sickling activates acid sphingomyelinase (SMase), which reduces this stress by converting membrane sphingomyelin to ceramide. This process can result in the production of sphingolipid-rich microparticles derived from the RBC membrane that can be secreted and interact with other cells in circulation (Bianco et al., 2009). Microparticles have been shown to be elevated in steady state in those with SCD and from basal levels during vaso-occlusive crises (Shet et al., 2003).

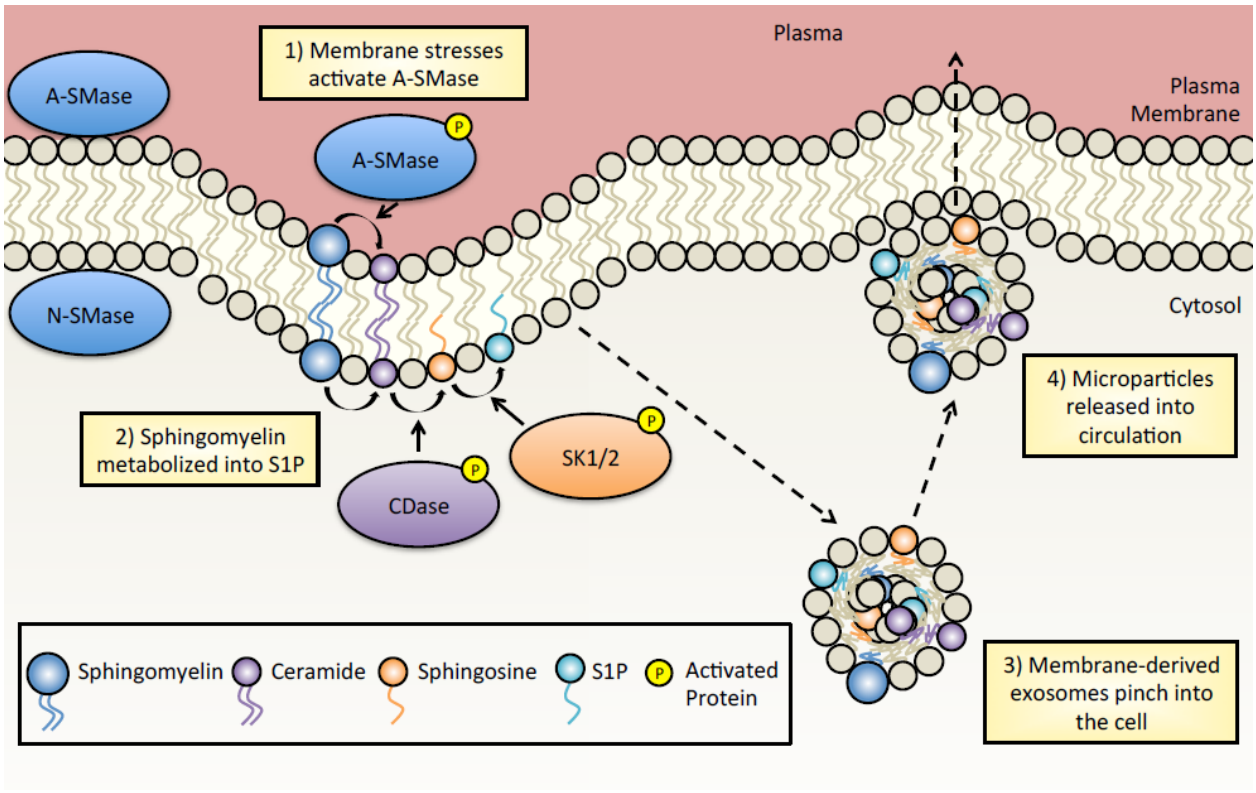

Figure 2. Schematic of sphingolipid metabolism and microparticle generation in SS RBC. When RBC undergo reversible sickling cycles, their membranes curve, introducing membrane stresses caused by the closer interaction of lipids. This increased membrane force activates acid sphingomyelinase (A-SMase) on the outer leaflet of the plasma membrane (1). Acid SMase hydrolyzes sphingomyelin to form ceramide which has a smaller head group and can cause an inward curvature of the membrane which reduces membrane stresses. Sphingomyelin can be further metabolized into sphingosine and S1P with alkaline ceramidase (CDase) and Sphingosine Kinase (SK1/2), respectively (2). Membrane budding results in the formation of membrane-derived exosomes (3), containing sphingolipids and proteins, which are internalized into the cell and subsequently released into circulation through secretion or hemolysis as microparticles (4).

The synthesis and metabolism of sphingolipids have been described in great detail (Hannun et al., 2001; Peest et al., 2008), but it is not understood under what conditions sphingolipid metabolism will be altered in diseases like sickle cell disease and how this contributes to the disease state. This work determined that sphingolipid metabolism is dysregulated in SCD through the quantification of the expression and activity of acid sphingomyelinase and several other enzymes in this pathway and the levels of S1P and sphingosine in SCD and non-SCD RBCs and microparticles. In addition, THP-1 monocytes and macrophages as well as primary peripheral blood mononucleated cells isolated from donors were treated with RBCs, microparticles, and S1P, and it was demonstrated that these compounds increase the adhesion of myeloid cells. These results suggest a novel pathway through which RBC sickling causes sphingolipid metabolism to be dysregulated in SCD, inducing the production of sphinglipid-rich microparticles that interact with myeloid cells in circulation and increase their adhesion at sites of clotting. This has significant implication for studying the origins and potential pharmacological therapies for vaso-occlusion.

CHAPTER 2

LITERATURE REVIEW

Sickle cell disease (SCD) is a blood disorder caused by a point mutation in the gene for hemoglobin. Defective hemoglobin results in sickling of red blood cells (Embury, 1986), which increases clotting because the misshapen cells are more likely to be caught in smaller vessels and capillaries (Conran et al., 2009; Hebbel et al., 1980). Monocytes derived from sickle cell blood have been shown to be more activated than normal monocytes (Belcher et al., 2000), and presumably macrophages may be more activated as well as they are derived from monocytes. Activation makes these cells more adherent, further contributing to inflammation and vaso-occlusion, which in extreme cases can ultimately result in organ failure and death (Belcher et al., 2000).

Sphingolipids are minor components of the cell membrane that can play a key role in membrane structure (Piccinini et al., 2010). Sphingolipids tend to aggregate and form lipid "rafts" in the cell membrane and alter its structure through the application of curvature stress (van Meer et al., 2008). In these locations, conversion of membrane sphingomyelin to ceramide by acid sphingomyelinase (SMase) can result in the production of microparticles (MPs) that can be secreted and interact with other cells in circulation (Bianco et al., 2009). Microparticles are important signaling molecules for innate immunity and have been shown to contain high levels of bioactive lipids like sphingosine 1-phosphate (Ratajczak et al., 2006).

Sphingosine 1-phosphate (S1P) is an anti-inflammatory sphingolipid that is involved in the regulation of lymphocyte traffic and many other cellular processes (Hughes et al., 2008). S1P is extremely important in regulating cell physiology, as evidenced by lethality in mice unable to produce S1P (Olivera et al., 2013). Red blood cells (RBCs) are known reservoirs for S1P;

however, S1P is present at low concentrations elsewhere in the body (Peest et al., 2008), suggesting that this gradients is significant in the ability of S1P to act with a high degree of specificity in regulation (Olivera et al., 2013).

S1P synthesis and metabolism pathways are well defined (Peest et al., 2008), but the role of S1P in sickle cell disease is not clear. This review will examine S1P metabolism and regulation of cell physiology, discuss how these results can be applied to the sickle cell disease state, and establish the gap that remains in understanding how altered sphingolipid metabolism may facilitate vaso-occlusion and inflammation in SCD.

S1P Metabolism and the Formation of S1P Gradients

The importance of S1P in regulating physiology is supported by the shown lethality of a double knockout of the genes for sphingosine kinase 1 and 2, the enzymes that phosphorylate sphingosine to make S1P (Olivera et al., 2013). S1P is present at varied concentrations throughout the body *in vivo,* suggesting that these gradients are significant in the ability of S1P to act with a high degree of specificity in regulation (Olivera et al., 2013).

S1P gradients are formed and maintained in part due to differential but ubiquitous metabolism of S1P by different types of cells, including HEK293, Jurkat, LK35.2, HB98, and HTC4 cells, and varying locations of these cells in the body (Olivera et al., 2013; Peest et al., 2008). S1P lyase, which degrades S1P to sphingosine, appears to play a significant role in maintaining the S1P gradient, as shown by the increased accumulation of S1P in serum and tissue in mice when the Sgpl1 gene was deleted (Peest et al., 2008). Specifically, Peest et al. (2008) concluded that S1P lyase is important for the clearance of *intracellular* S1P; however, clearance of *extracellular* S1P through dephosphorylation to sphingosine and subsequent metabolism occurs independently of S1P lyase, ceramide synthase, and sphingosine kinase.

Peest et al. (2008) concluded that the ability of all cell types tested (including HEK293, Jurkat, LK35.2, HB98, and HTC4 cells) to clear exogenous S1P supports a ubiquitous mechanism present in all cells for keeping extracellular S1P and sphingosine levels low, with one exception: blood acts as a reservoir for S1P. Specific focus on the S1P gradient in sickle cell disease will be valuable because SCD is a disorder of the blood.

S1P as a Regulator of Cell Physiology

In endothelial cells, S1P functions in survival, migration, and nitric oxide synthesis and can also act to regulate the vascular barrier of endothelium by rearranging their cytoskeletons (Cuvillier et al., 1996). Specifically, deletion of the transporter protein gene Spns2 in endothelial cells resulted in decreased levels of S1P in plasma, suggesting that endothelial cells play a significant role in S1P secretion and maintenance of the S1P gradient via transporter proteins. Aoki et al. suggest that S1P plays a role in maintaining integrity of the vascular barrier of endothelial cells in part by mediating the redistribution of endothelial integrins from the luminal to the basal surface of the cells (2007).

The role of S1P in contributing to monocyte adhesion to endothelial cells is disputed because S1P has been shown to both increase and decrease adhesion and the expression of adhesion molecules in endothelial cells depending on whether the cells are stimulated with TNF-a. Aoki et al. found that S1P pretreatment of endothelial cells inhibited monocyte adhesion independently from the expression of ICAM-1, VCAM-1, and E-selectin and was prevented by blocking S1P1 and S1P3 receptors as well as several proteins. Inhibition of integrins a5b1 and avb3 prevented monocyte to endothelial cell adhesion (Aoki et al., 2007).

Hughes et al. (2008) demonstrate that S1P can facilitate the phenotypic change from inflammatory to anti-inflammatory in macrophages largely through activation of the receptor

S1P1. At a concentration near what is seen in blood (500 nM), S1P was shown to reduce the inflammatory effects of LPS by suppressing several inflammatory cytokines, including TNF-a, MCP-1, IL-12, COX-2, and MIP2 and enhancement of Arg I expression and reduced induction of iNOS, demonstrating an important point for any potential S1P therapies for sickle cell disease (Hughes et al., 2008).

Cuvillier et al. (1996) demonstrated that S1P can reduce several characteristic responses of apoptosis in HL-60 and U937 cells, including intranucleosomal DNA fragmentation and typical changes in morphology, that were induced by C_2-ceramide treatment, sphingomyelinase treatment, and stimulation of sphingomyelinase through the ligands TNF-α and Fas. Stimulation of protein kinase C inhibited apoptosis induced by ceramide by increasing intracellular levels of S1P. An inhibitor of sphingosine kinase, the enzyme that produces S1P by phosphorylating sphingosine, was used and the previous decrease in apoptosis was not observed. These results suggest that S1P and ceramide play important roles in regulating programmed cell death (Cuvillier et al., 1996).

Gude et al. (2008) examined the role of S1P and SphK1 in apoptosis to determine if S1P could be a "come-and-get-me" signaling molecule for macrophages. Treatment of Jurkat and U937 leukemia cells with the SphK1 inhibitors DMS and DHS induced apoptosis and increased the expression of SphK1, as did treatment with the proapoptotic drug doxorubicin, and resulted in a more than 3-fold increase in S1P secretion. These effects were significantly reduced by apoptosis inhibitor ZVAD. S1P was shown to act as a chemoattractant for primary monocytes and macrophages, maximally at 10 nM and 1 nM, respectively (Gude et al., 2008).

The recruitment of anti-inflammatory monocytes in addition to phenotypic changes to anti-inflammatory states may be mediated by the receptors $S1P_3$ and $S1P_1$. Awojoodu et al.

(2013) showed that treatment of inflamed tissue in mice with FTY720, an $S1P_{1/3}$ agonist, resulted in increased recruitment of anti-inflammatory monocytes to the targeted tissue through increased anti-inflammatory and reduced pro-inflammatory cytokine secretion, which was not observed in $S1P_3$ knockout mice. It was also found that anti-inflammatory monocytes expressed more $S1P_3$. Hughes et al. (2008) found that S1P facilitates the phenotypic change from inflammatory to anti-inflammatory in macrophages derived from mouse bone marrow largely through activation of the receptor $S1P_1$ by suppressing several inflammatory cytokines, including TNF-a, MCP-1, IL-12, COX-2, and MIP2, enhancement of Arg I expression, and reduced induction of iNOS.

Microparticles

A new area of research that has arisen recently involves microparticles. Microparticles (MPs) are important signaling molecules for innate immunity that have been shown to be derived from the cell membrane of dying or activated cells (Gauley and Pisetsky, 2010) and to have significant levels of bioactive sphingolipids like S1P (Ratajczak et al., 2006). Conversion of membrane sphingomyelin to ceramide by acid sphingomyelinase (SMase) can result in microparticle production (Bianco et al., 2009).

Gauley and Pisetsky found that in response to several Toll-like receptor ligands, MP release increased, and this release was linked to (1) NO production through studies inhibiting iNOS, which impeded MP production, and (2) incubation with NO donors, which increased MP production (2010). NO production is associated with macrophage activation (Green et al., 1990; Nathan, 1997), so microparticle production may act as a key intermediate in this process.

CHAPTER 3

MATERIALS AND METHODS

Density Fractionation of Blood and Characterization of Microparticles

Whole blood samples were obtained from males and females homozygous for sickle (SS) or normal (AA) hemoglobin through the Sickle Cell Foundation of Georgia. Donors on hydroxyurea, chronic transfusion, or who had experienced a recent crisis were excluded from this study.

Isolation of Peripheral Blood Mononuclear Cells and Red Blood Cells

Whole blood samples were diluted 1:1 in ice-cold PBS and centrifuged against a Ficoll-Paque density gradient (density: 1.077g/mL; GE Healthcare) for 30 minutes at 400 RCF at 4˚C to allow separation of the plasma, buffy coat layer, and packed red blood cells. After centrifugation, blood plasma and packed red cells were collected. Peripheral blood mononuclear cells (PBMCs) were washed in PBS and pelleted by centrifugation at 300 RCF for 10 minutes. Contamination of red blood cells in the PBMC layer was removed using red blood cell lysis buffer (0.83% ammonium chloride, 0.1% potassium bicarbonate, and 0.0037% EDTA) for 7 minutes followed by washing three times in PBS.

RBC Density Fractionation

RBCs were separated into high and low density fractions according to a protocol by D'Alessandro et al. (2013). Briefly, 8 Percoll solutions of varying density were made with Percoll, BSA, Hepes, NaCl and KCl and stacked in order of decreasing density, from bottom to top, in Beckman ultra-clear™ tubes $^{9}/_{16}$ x $3^{1}/_{2}$ in. (14 x 89 mm). The stacked gradient was pre-centrifuged at 20,000 RCF for 20 minutes. 300µL of packed RBCs were added to 1.5mL of 5mM Na_2HPO_4, 154mM NaCl, 5mM Glucose and 1mM PMSF and centrifuged at 200 RCF for 10 minutes at 4C. The supernantant was discarded, and this process was repeated twice. The cells were resuspended in 1.5mL of 95% glucose. The RBC sample was loaded slowly on top of the Percoll gradient and centrifuged at 41,000rpm for 30 minutes using a Beckman SW 41 Ti rotor. The highest and lowest density RBC fractions were collected using a syringe and washed in PBS with 0.8% NaCl.

Microparticle Harvest and CFSE Staining

MP were harvested by ultracentrifugation of AA or SS blood diluted 10-fold in PBS. P3 MP were obtained by ultracentrifugation of diluted blood at 2000 RCF for 20 minutes at 4°C. The supernatant was ultracentrifuged at 3000 RCF for 10 minutes at 4°C, and the resulting supernatant was ultracentrifuged at 37,000 RCF for 1 hour at 4°C. The supernatant was removed, and the MP were resuspended in PBS. P2 MP were obtained by ultracentrifugation of diluted blood at 10,000 RCF for 15 minutes at 4°C. The supernatant was spun at 200,000 RCF for 1 hour at 4°C to obtain P4 MP.

MP were stained with CFSE at a 1:1 dilution for 20 minutes at room temperature followed by ultracentrifugation at 16,000 RCF for 20 minutes at 10°C. The supernatant was removed and the MPs were resuspended in PBS.

Flow Cytometry for Microparticle Quantification

Plasma and packed RBC were fractionated and isolated from donors as described above and incubated with antibodies against CD41 (catalog #Ab19690, Abcam), Glycophorin A (catalog #Ab91163, Abcam) and Annexin V (catalog #640906, Biolegend). Cells were counted with Accucheck counting beads (catalog #PCB100, Life Technologies) and analyzed on a BD FACS Aria flow cytometer.

AA/SS Blood Microparticle Characterization

SEM Sample Preparation

Cells fixed with 2.5% glutaraldehyde fixative in 0.1 M cacodylate buffer (pH 7.4) were placed on a Poly-L-Lysine coated silicon wafer (5 x 5 mm), washed with same buffer and then post fixed in 1% osmium tetroxide with 1.5% potassium ferrocyanide in 0.1 M cacodylate buffer for one hour. Cells were subsequently rinsed 2 or 3 exchanges of de-ionized water. This was followed by dehydration through an ethanol series ending with three exchanges of 100% absolute ethanol. The samples were then placed into individual ventilated processing vessels in fresh absolute ethanol and placed into a Polaron E3000 critical point drying unit wherein the ethanol was exchanged for liquid CO_2. The liquid CO_2 was eventually brought to its critical point of 1073 psi at 31°C and allowed to slowly vent. The dried samples were then secured to labeled aluminum SEM stubs and coated with approximately 20 nm of chromium using an Denton DV-602 turbo magnetron sputter coater (Denton Vaccum, LLC., Moorestown, NJ). Sample were then viewed with a Topcon DS130F field emission scanning electron microscope using 5 kV accelerating voltage.

TEM Sample Preparation

5 µl microparticle suspension was place on a 400 mesh carbon coated copper grid that had been made hydrophilic by glow discharge. After 5 minutes, the grid was rinsed by briefly touching the sample side with one drop of distilled water. The residual water on grid was then removed by dragging the side of grid on a piece of filter paper. For negative staining, 5 µl 1% aqueous phosphotungstic acid (pH 6.5) was applied onto grid immediately after water removal, and then removed as described above after 30 seconds. The grid was let completely dry before viewing on a JEOL JEM-1400 transmission electron microscope (JEOL Ltd, Tokyo, Japan) equipped with a Gatan US1000 2k x2k CCD camera ((Gatan, Inc., Pleasanton, CA).

Size Quantification

MP size was evaluated by taking perpendicular measurements in ImageJ of MP diameter from TEM images. The average of the two measurements was taken and converted from pixels to nanometers using the length in pixels of the scale bar. The average diameter for each group (SS and AA P2, P3, and P4 MP) was obtained by taking the average of the diameter from each image.

Protein Expression

SMase Expression

Neutral and acidic sphingomyelinase (SMase) activity were measured with a sphingomyelinase fluorometric assay kit (catalog # 10006964, Cayman Chemical Company). For neutral SMase activity, the reaction was performed in a neutral buffer at a pH of 7.4. For acidic SMase activity, the reaction was performed in an acidic buffer at a pH of 5. Briefly, 10µL of

samples (plasma, whole blood or RBC) were combined with alkaline phosphatase and a fluorometric sphingomyelin substrate. The reaction involving SMase hydrolyzes sphingomyelin to form ceramide and phosphorylcholine. Alkaline phosphatase hydrolyzes phosphorylcholine to form choline. Choline is then oxidized by choline oxidase to produce betaine and H_2O_2. H_2O_2, in the presence of horseradish peroxidase, reacts with ADHP to yield fluorescent resorufin, which was measured on a plate reader at an excitation wavelength of 535nm and emission wavelength of 590nm after 30 minutes.

Acid sphingomyelinase expression was measured with a sphingomyelinase absorbance ELISA assay kit (catalog # SEB360Hu, USCN Life Science). 10µL sample was loaded into wells in a 96 well plate ELISA kit pre-coated with a monoclonal antibody against acid SMase (catalog #MAB360Hu22, USCN Life Science). Expression was measured by reading the absorbance at 450nm.

Ceramidase Expression

Alkaline ceramidase (ACER1) expression was measured with a ceramidase absorbance ELISA assay kit (catalog # CSB-EL001151HU, CUSABio). 10µL sample was loaded into wells in a 96 well plate ELISA kit pre-coated with a monoclonal antibody against alkaline ceramidase (ACER1). Expression was measured by reading the absorbance at 450nm.

SK1/2 Expression

Sphingosine kinase 1 and 2 expression were measured by western blotting using antibodies against sphingosine kinase 1 (catalog #1000-6822, Caymen Chemical Company) or sphingosine kinase 2 (catalog #AB37977, Abcam). An equal amount of protein was loaded onto

the gels and near IR dyes were used to stain the relevant bands. Expression is expressed as relative fluorescent units.

Lipid Extraction and S1P/Sphingosine Quantification

Lipids were extracted following a protocol from Shaner et al. (2009). Briefly, 15-150µL of whole blood, plasma or RBC was transferred into 13 × 100 mm borosilicate tubes with a Teflon-lined caps (catalog #60827-453, VWR, West Chester, PA). 500µL of CH_3OH, 250µL of $CHCl_3$ and 10µL of C17 Sph+C17 S1P (Cayman Chemicals) internal standard were added to the sample and the samples were sonicated at room temperature for 30 seconds. The single phase mixture was incubated at 48°C overnight in a water bath and cooled before 75 µl of 1 M KOH in CH_3OH was added. Samples were sonicated for 5 minutes and shaken in a 37°C water bath for 2 hours. Samples were cooled and glacial acetic acid was added to bring the extract to neutral pH. Samples were centrifuged to remove the insoluble residue and the supernatant was collected. The supernatant was placed in glass vials and dried for 6 hours using a nitrogen blow down system. The dried residue was reconstituted in 300µL of methanol and analyzed using a Shimadzu LC-10 AD VP binary pump system coupled to a Perkin Elmer Series 200 autoinjector coupled to a 4000 quadrupole linear-ion trap (QTrap) LC-MS/MS system for S1P and sphingosine quantification.

Cell Culture

THP-1

Human THP-1 monocytes (ATCC) were maintained in RPMI-1640 medium (Sigma-Aldrich) supplemented with 10% fetal bovine serum, 1% penicillin-streptomycin, and 0.05 mM

β-mercaptoethanol at 37°C in a 5% CO_2 atmosphere. All cells were maintained and all incubations were performed under these conditions unless mentioned otherwise

Macrophage Polarization

THP-1 monocytes were seeded on PDL-coated coverslips and differentiated to M0 macrophages with 100 nM phorbol myristate acetate (PMA) for 72 hours. M0 macrophages were subsequently polarized to M1 macrophages with 5 mg/mL LPS and 10 μg/mL IFN-γ or to M2 macrophages with 454.5 ng/mL IL-4 for 24 hours.

HUVEC

HUVEC (ATCC) were maintained in CS-C Serum Supplemented Medium (Sigma-Aldrich) in gelatin-coated flasks at 37°C in a 5% CO_2 atmosphere. After the cells were 80% confluent, they were passaged into new media. GFP-HUVEC were obtained through transfection with a EF1α-eGFP vector and were a kind gift of the Platt laboratory at the Georgia Institute of Technology.

Cell Staining, Fixation and Confocal Microscopy

As appropriate, monocytes were stained with 10 μM Calcein AM (Life Technologies) for 1 hour before co-incubation. For assays measuring adherence, adherent cells were washed twice with PBS and were fixed with 4% paraformaldehyde for 20 minutes. Cells were stained with Hoechst (Life Technologies) in PBS and mounted with VECTASHIELD Mounting Medium (Vector Laboratories). Slides were imaged using a Zeiss 700 laser scanning confocal microscope.

THP-1 and HUVEC Co-Culture/Adhesion

GFP-HUVEC were seeded in an 8 chamber slide (3 x 10^5 cells/chamber) and grown to confluence. THP-1 were co-incubated with HUVEC under the conditions described below. The chambers were washed gently and the nonadherent THP-1 monocytes were removed and counted using a hemocytometer. Adherent cells were fixed and stained as described above.

S1P Treatment

HUVEC and THP-1 monocytes received vehicle or 1μM S1P treatment for 1 hour. Cells were washed with media, and HUVEC were co-incubated with 1 x 10^5 THP-1 monocytes for 4 hours.

RBC Co-Culture

THP-1 monocytes were incubated with red blood cells derived from AA or SS donors at a 1:10 ratio of THP-1 monocytes:RBCs for 18 hours. HUVEC were co-incubated with 1 x 10^5 THP-1 monocytes and 1 x 10^6 RBCs for 4 hours.

Quantification for Adhesion

Confocal images of each chamber were used to obtain the ratio of adherent THP-1 monocytes:HUVEC for the adhesion studies. The number of each cell type present in each image was quantified based on the morphology of the nuclei and the DAPI, GFP, and Calcein AM stains. ImageJ was used to quantify the nuclei present in at least 5 fields of view from each chamber. The live counts obtained for non-adherent THP-1 monocytes were used to calculate the percent of adherent cells based on the initial seeding density of THP-1 monocytes.

AA/SS RBC Microparticle Internalization

THP-1 monocytes were seeded at a density of 2 x 10^5 cells/well on PDL-coated coverslips and polarized to M0 macrophages as described previously. CFSE-stained SS or AA MPs were added at a density of 1 x 10^6/well. After 30 or 120 minute incubations, the conditioned media was removed from each well and uninternalized MPs were quantified as described above with a BD FACS Aria flow cytometer. M0 macrophages were washed with PBS and permeabilized with 0.5% Triton (Sigma Aldrich) for 5 minutes, fixed as described above, and stained with rhodamine phalloidin (Life Technologies) at a concentration of 5 µL/1 mL sample. Cells were washed and mounted as described above.

Macrophage Microparticle Treatment and Luminex Cytokine Secretion

THP-1 monocytes were seeded at a density of 2 x 10^5 cells/well on PDL-coated coverslips and polarized to M0, M1, and M2 macrophages as described previously. After treatment of the macrophages with SS MP for 1, 2, or 6 hours, the conditioned media was removed and a protease inhibitor was added at a 1:100 dilution. RIPA buffer was added to each well, and the cells were removed by scraping and were left on ice for 20 minutes. The cell lysate was centrifuged at 200 RCF and the supernatant was combined with a protease inhibitor at a 1:100 dilution. Samples were stored at -80^{o}C. Anti-inflammatory and inflammatory cytokines were assessed by a Milliplex MAP Human Cytokine/Chemokine Premixed 42 Plex Assay (catalog # MPXHCYTO60KPMX42, Millipore) on the Luminex platform as per the manufacturer's instructions.

RBC Microparticle Generation with Amitriptyline

In vitro

Packed RBC were isolated from SS donors as described above. Amitriptyline (catalog #A8404, Sigma) was prepared at four different concentrations in sterile PBS. 100,000 cells were placed in wells of a 24 well plate in the presence of the four different concentrations of amitriptyline and incubated at 37°C for 1 or 24 hours. Flow cytometry was used to quantify RBC and microparticles as described above.

In vivo

Wild-type C57BL/6 mice were obtained from The Jackson Laboratories; Heterozygous AS and homozygous SS mice were initially obtained from the sickle transgenic breeding colony at Georgia Institute of Technology. Townes' model sickle transgenic mice were heterozygous (AS) or homozygous (SS) for the sickle mutation. To determine sickle status, whole blood was obtained from each animal via retro-orbital capillary draws. Whole blood was lysed with distilled water and diluted 1:1 in a 50% glycerol solution. Blood samples were then run on a Native PAGE gel and hemoglobin was visualized using a liquid tetramethylbenzidine stain (34% EtOH, 32% liquid 3,3',5,5'-tetramethylbenzidine, 2% acetic acid, 1% H2O2); sickle hemoglobin has a smaller electrophoretic migration distance than normal hemoglobin. Mice in all studies were male, 8–12 wk old, and weighed 18–25 g. Amitriptyline was injected at 4 different doses via intraperitoneal administration and blood was collected via retro-orbital capillary draws. RBC and microparticles in blood were quantified as described above with a BD FACS Aria flow cytometer. All surgical procedures and animal care protocols were approved by the Georgia Institute of Technology Animal Care and Use Committee.

CHAPTER 4

RESULTS

Dysregulation of sphingolipid metabolism in SCD

A sphingomyelinase fluorometric assay kit was used to measure neutral and acid sphingomyelinase activity in AA and SS plasma and RBC. Sphingomyelinase converts sphingomyelin to ceramide (Figure 2). Neutral sphingomyelinase activity was low and was not significantly different in AA and SS plasma (Figure 3A). A slight elevation was seen in neutral sphingomyelinase activity in SS RBC (Figure 3B). Acid sphingomyelinase expression did not differ in RBC or plasma for SS vs. AA (Figure 3E); however, acid sphingomyelinase activity was elevated in SS RBC and plasma (Figure 3C and 3D) as well as in high density (sickled) RBC in comparison to low density RBC (Figure 3F). Acid sphingomyelinase activity was approximately 10-fold higher in RBCs than in plasma (Figure 3C and 3D).

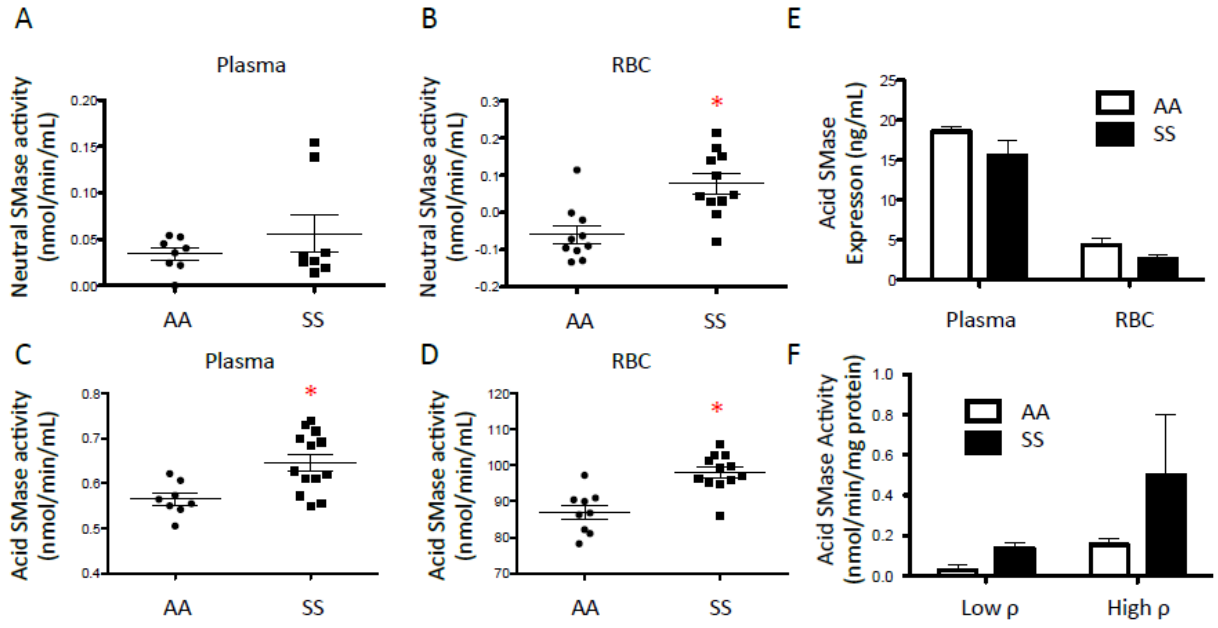

Figure 3. Acid and Neutral Sphingomyelinase activity in AA and SS RBC and plasma. Donor blood was harvested and fractionated in a Ficoll density gradient to separate plasma and RBC. A plate based assay for sphingomyelinase activity was performed at a neutral pH on

plasma (A) and RBC (B). Neutral sphingomyelinase activity was very low or undetectable in both plasma (A) and RBC (B). SMase activity, while still low, was significantly increased in SS RBC (B) relative to AA RBC. This is likely due to residual (sub-optimal) acid SMase activity at neutral pH or activation of neutral SMase. A plate based assay for acid sphingomyelinase activity was performed on plasma (C) and RBC (D). Acid sphingomyelinase activity was elevated in both plasma and RBC from SCD donors relative to non-diseased donors. A plate based ELISA for sphingomyelinase expression was performed on plasma and RBC (E). Sphingomyelinase expression was not altered in the plasma (left) or RBC (right) of those living with SCD. Packed RBC from AA and SS donors were stacked onto Percoll density discontinuous layers and spun with ultracentrifugation to separate two distinct density (high and low) fractions of cells. F) High density RBC had higher sphingomyelinase activity than low density RBC. Low density RBC from SS donors had much higher sphingomyelinase activity than low density AA cells and high density RBC from SS donors had much higher sphingomyelinase activity than high density AA cells. Morphological differences were apparent between the four fractions (G) Scale bar = 5μm. * $p < 0.05$ measured in a t-test.

Acid ceramidase and sphingosine kinase 1 and 2 expression were quantified using ELISAs. Ceramidase converts ceramide to sphingosine, and sphingoskine kinase phosphorylates sphingosine to produce S1P (Figure 2). Acid ceramidase 1 expression is unaltered in SS RBC (Figure 4A) but is elevated in SS plasma (Figure 4B). The expression of sphingosine kinase 1 was unaltered, but sphingosine kinase 2 expression was significantly elevated in SS RBC and plasma (Figure 4C-4F). HPLC was used to quantify S1P and sphingosine in whole blood, RBC, and plasma. S1P and sphingosine were significantly elevated in SS whole blood (Figure 4G), plasma (Figure 4H), and RBC (Figure 4I). S1P and sphingosine levels were over 10-fold higher in RBC than plasma (Figure 4H and 4I). Overall, S1P was present at a higher concentration than sphingosine.

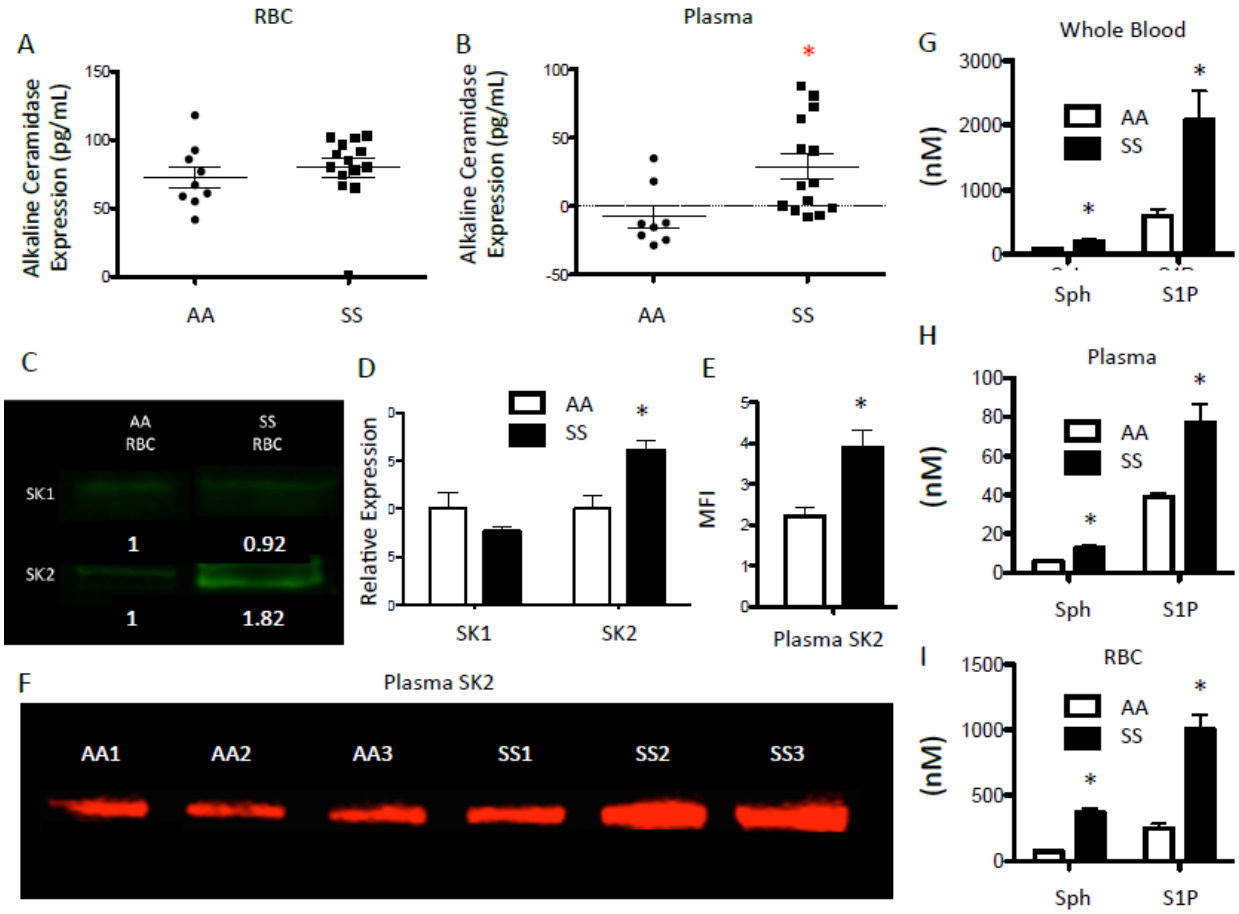

Figure 4. Alkaline ceramidase, sphingosine kinase 2, S1P and sphingosine elevated in SCD. Donor blood was harvested and fractionated in a Ficoll density gradient to separate plasma and RBC. A plate based assay for alkaline ceramidase (ACER1) expression was performed on RBCs (A) and plasma (B). ACER1 expression was not altered in SCD RBC. ACER1 was not detected in the plasma of those without SCD but was elevated in the plasma of those with SCD. RBC were fractionated from donor blood and lysed in RIPA buffer. C) Western blotting shows expression of both SK1 and SK2, but only SK2 was visibly elevated in SS RBC. D) Relative fold changes in SK1 and K2 expression reveal a significant increase in SK2 expression in SS RBC. E-F) Donor plasma was assessed for SK2 expression and plasma from those living with SS had significantly more SK2, relative to AA, suggesting that SK2 is secreted during SCD. Lipids were extracted from donor samples and sphingosine and S1P levels in whole blood (G), plasma (H) and RBC (I) was quantified with HPLC-MS. * $p < 0.05$ measured in a t-test.

Monocyte adhesion is enhanced by S1P pre-treatment and by co-incubation with SCD RBCs

THP-1 monocytes and HUVECs were co-incubated after treatment with S1P. When HUVECs were treated with S1P, no change in adhesion was seen in comparison to the control after a 4 hour incubation. Adhesion increased over 4-fold when THP-1 monocytes were treated with S1P (Figure 5A), as seen in Figure 5C. A significant increase in monocyte adhesion was seen in as little as 4 hours (Figure 5B).

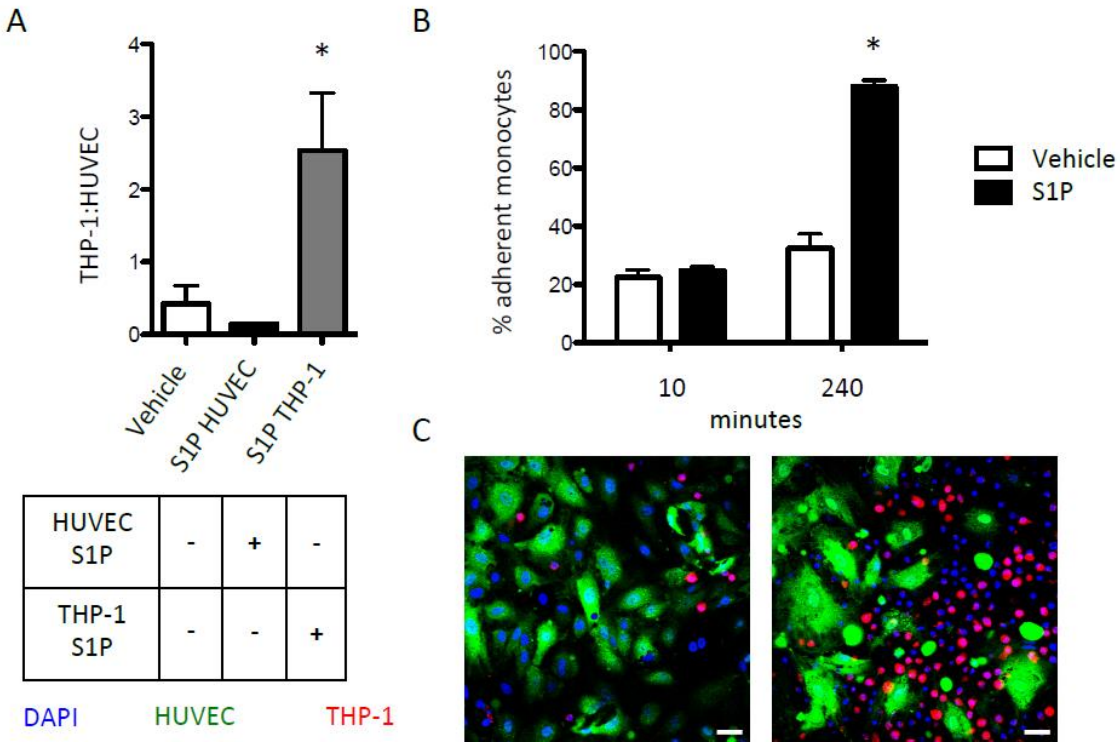

Figure 5. S1P treatment of monocytes enhances endothelial adhesion. A) HUVEC were grown to confluence and co-incubated with THP-1 monocytes for 4 hours after 1 hour vehicle treatment, 1μM S1P treatment of HUVEC or 1μM S1P treatment of monocytes. S1P treatment of monocytes significantly enhanced the adherent monocyte : endothelial cell ratio after 4 hours. B-C) THP-1 monocytes were treated with 1μM S1P and allowed to adhere to HUVEC for 4 hours. S1P treatment did not affect early adhesion but resulted in an increase in monocyte adhesion after 240 minutes (B). Representative confocal images (C). *Scale bar = 10μm.* * $p < 0.05$ measured in one-way ANOVA or t-test.

AA RBCs or SS RBCs (sickled RBCs are circled in red) were incubated with THP-1 monocytes for 18 hours (Figure 6A), followed by a 4 hour co-incubation with HUVEC. Adhesion was increased almost 4-fold for monocytes treated with SS RBC in comparison to AA RBC (Figure 6B), as seen in Figure 6C.

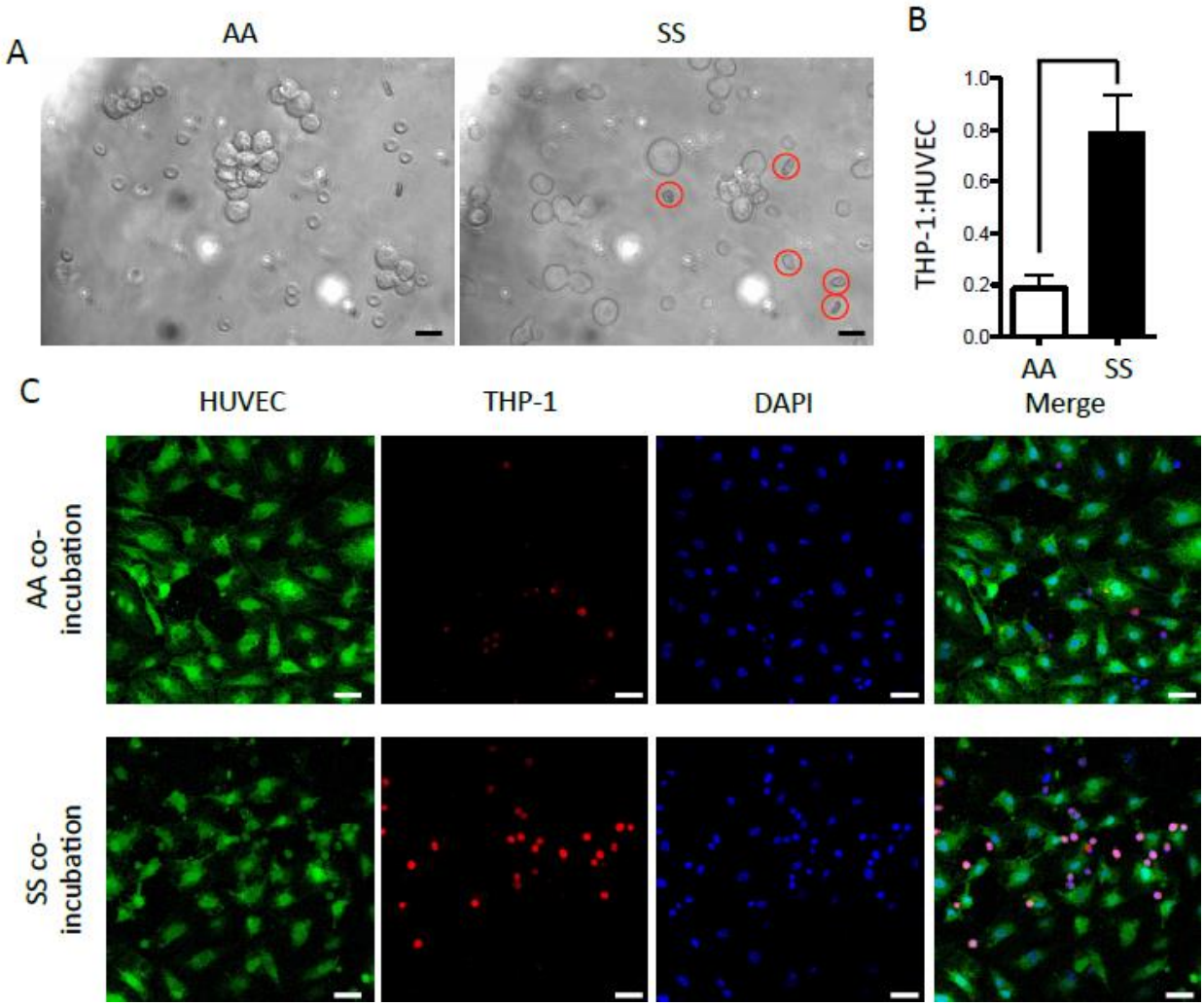

Figure 6. Co-incubation of SS RBC and monocytes enhances endothelial adhesion. A) AA (left) or SS (right) RBC were co-incubated with THP-1 monocytes (10:1) for 18 hours. Sickle RBC (red circles) are visible. B-C) Co-incubation of THP-1 monocytes with SS RBC significantly enhanced monocyte:HUVEC ratio after 4 hour adhesion (B). Representative images (C) show enhanced THP-1 monocytes (red cells) adhered to a HUVEC (green) monolayer. *Scale bar = 10μm.* $p < 0.05$ measured in t-test.

Microparticles are elevated in SCD and modulate cytokine production in myeloid cells

Microparticles in AA and SS plasma and RBC were quantified using flow cytometry (Figure 7A-D). Microparticles were slightly elevated in SS plasma (Figure 7B) and were significantly elevated by almost 2-fold in SS RBCs (Figure 7D). Microparticles were separated by size using differential ultracentrifugation and were imaged using TEM (Fig 7E). The small microparticles (P4) had an average diameter of approximately 200 nm, and large microparticles (P2) had an average diameter of approximately 300 nm. The overall population of microparticles had an average diameter of approximately 200 nm. HPLC was used to quantify the lipid profile of the microparticles. In SS microparticles, sphingosine and S1P (Figure 7F) were elevated by over three-fold, and ratio of ceramide to sphingomyelin (Figure 7G) was significantly elevated as well.

Microparticles were observed to interact with macrophages. SS microparticles were internalized by M0 macrophages in as little as 30 minutes (Figure 7H). Treatment of M0, M1, and M2 macrophages with SS microparticles increased inflammatory cytokine production and secretion. Specifically, MIP-1a, TNF-α, and IL-6, three cytokines associated with SCD vaso-occlusive crises (Keikhaei et al., 2013), were elevated in M0, M1, and M2 macrophages in comparison to untreated cells (Figure 7I and Figure 7J). Notably, IL-6 was the cytokine that was most elevated when normalized to non-treated cells, with the highest fold change observed in M0 and M2 macrophages.

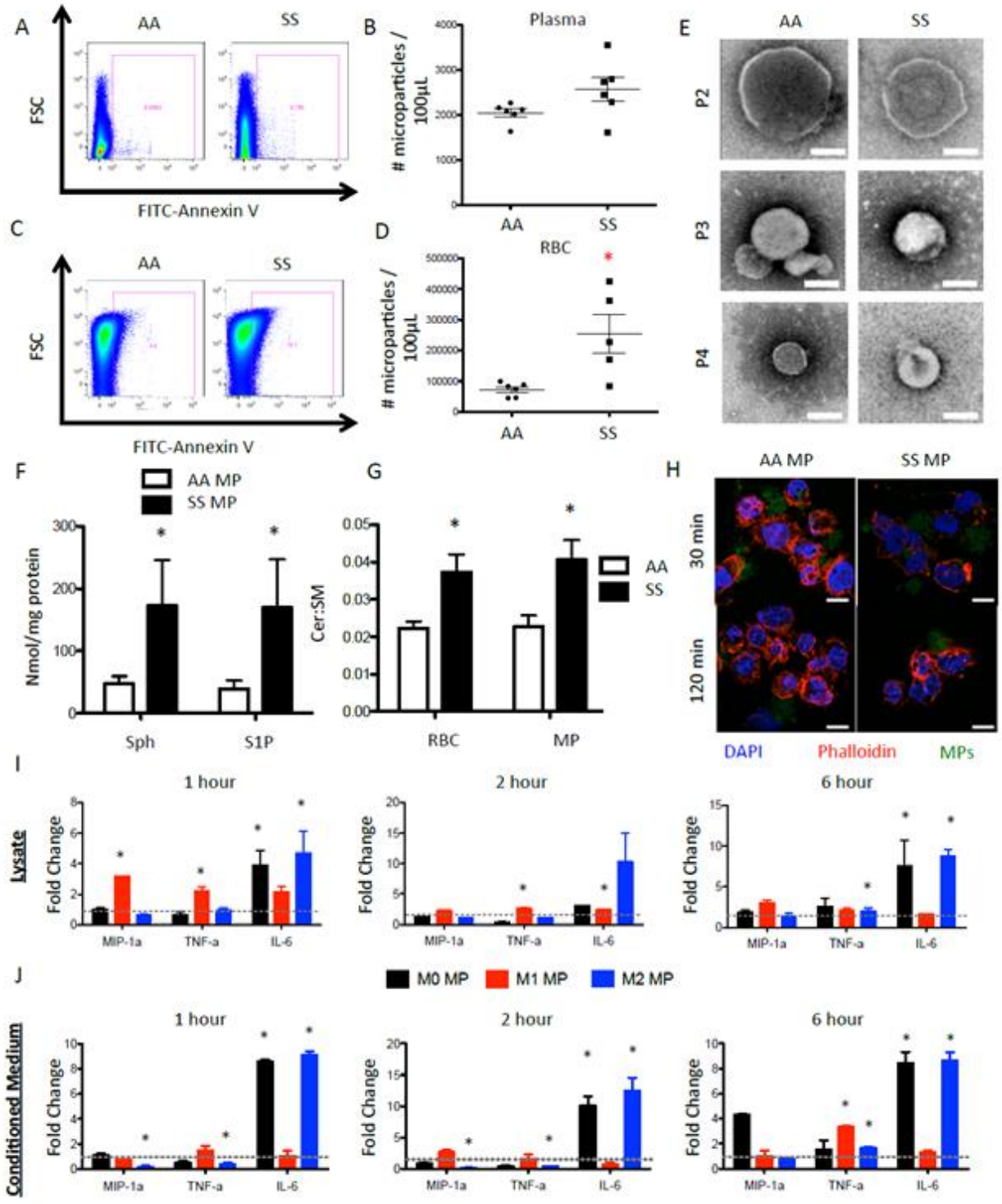

Figure 7. RBC derived microparticles are significantly increased in SCD and are internalized by macrophages and enhance cytokine production. Donor blood was fractionated and microparticles were quantified in plasma and RBC via flow cytometry. A) Annexin-V^{+} microparticles were observed in the plasma of AA (left) and SS (right) donors. B)

Microparticle concentration was between 2000 and 2500 microparticles per 100μL plasma. C) Annexin-V^+ microparticles were observed in the RBC fraction of AA (left) and SS (right) donors. D) Microparticle concentration was around 100,000 per 100μL for AA RBC but significantly elevated (250,000 per 100μL) for SS RBC. Microparticles were harvested from packed RBC at three different serial ultracentrifugation speeds for one hour. E) TEM images were taken of microparticles harvested at 10,000 (P2), 37,000xg (P3) or 200,000xg (P4) for one hour. *Scale bar = 200nm.* F) P2 microparticles were around 300nm on average while P3 and P4 microparticles were around 200nm. G) P3 microparticles were labeled with CFSE and incubated with M0 THP-1 macrophages for 30 (top) or 120 (bottom) minutes. *Scale bar = 10μm.* Flow cytometry was used to quantify the number of particles internalized (H). A higher proportion of cells was internalized in 30 minutes than 120 minutes suggesting that microparticles can be internalized and subsequently secreted but there were no differences between AA and SS microparticles. I-J) SCD RBC-derived P3 microparticles were incubated with M0 (black), M1 (red) or M2 (blue) macrophages for 1 (left), 2 (middle) or 6 (right) hours. Microparticle incubation enhanced the production (I) and secretion (J) of inflammatory cytokines MIP-1a, TNF-a and IL-6 relative to untreated cells (dotted line). * $p < 0.05$ measured in t-test.

Inhibition of acid sphingomyelinase reduces the generation of microparticles *in vivo* in mice and *in vitro* in red blood cells

Microparticles were quantified by flow cytometry in packed SS RBCs treated with amitriptyline for 24 hours *in vitro*. Both the percent of microparticles out of total events and the ratio of microparticles to RBCs were reduced in a dose-dependent fashion, and this reduction was significant using 100 μM amitriptyline (Figure 8A-D). *In vivo*, 10 mpk amitriptyline reduced acid sphingomyelinase activity significantly after 24 hour treatment and reduced microparticle generation in comparison to control (Figure 8E and Figure 8F).

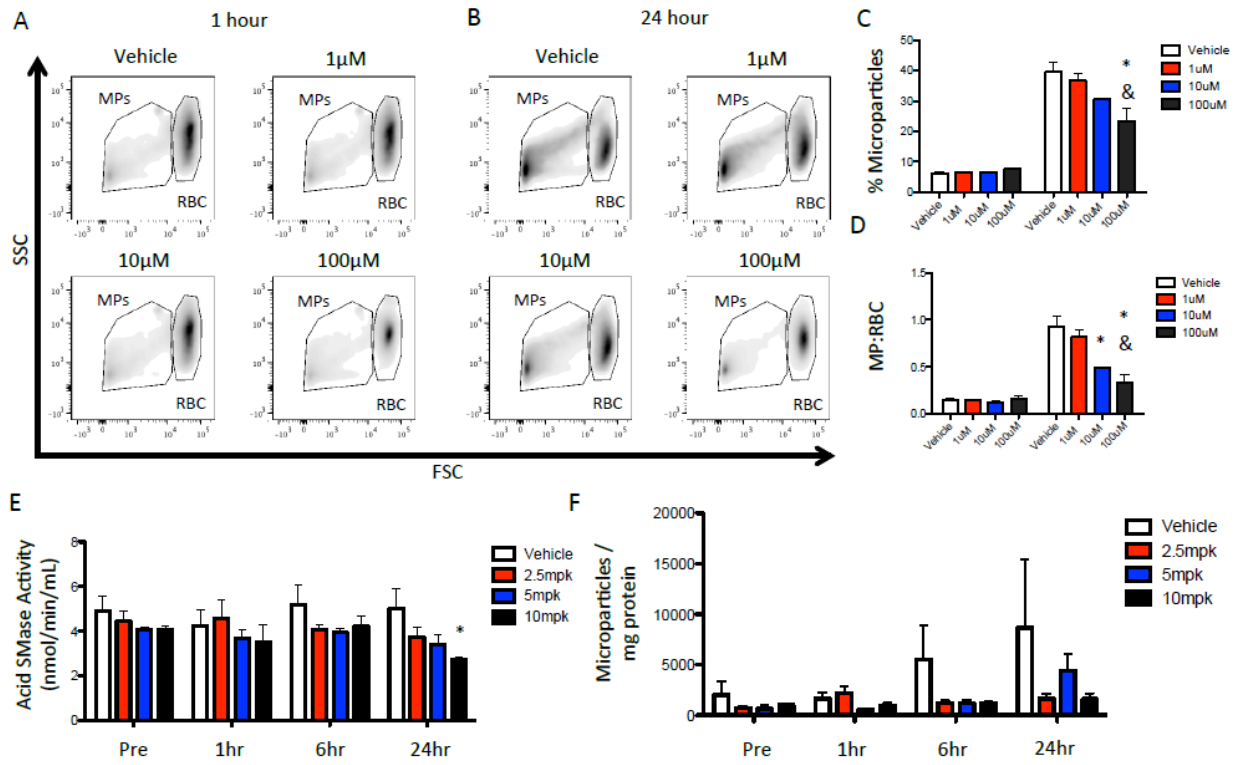

Figure 8. Amitriptyline reduces microparticle generation in RBC. A-B) Flow cytometry showing microparticles and RBC at 1 hour (A) and 24 hours (B). C-D) 100μM Amitriptyline significantly reduces the percentage of microparticles produced from SS RBC (C). 10 and 100μM Amitriptyline significantly reduces the proportion of microparticles produced from SS RBC (D). E) 10mpk Amitriptyline significantly reduces acid sphingomyelinase activity in C57/Bl6 mice 24 hours after injection. F) Amitriptyline reduces microparticle generation relative to vehicle treated groups as early as 1 hour after injection. * $p<0.05$ compared to vehicle, & $p<0.05$ compared to 1uM

CHAPTER 5

DISCUSSION

SCD is associated with severe vaso-occlusive crises initiated by RBC sickling (Conran et al., 2009; Hebbel et al., 1980). Belcher et al. (2000) note that myeloid cells are activated in the disease state, which contributes to vaso-occlusion through the increased adherence of these cells. Recent studies indicate that microparticles produced in SCD contribute to the activation of these cells (Mause and Weber, 2010; Tantawy et al., 2012). This work illustrates a connection between dysregulated sphingolipid metabolism and the pathology of vaso-occlusion in sickle cell disease through microparticle-mediated activation of myeloid cells and is suggestive of a pathway that may be open for pharmacological intervention.

Acid sphingomyelinase is associated with microparticle generation (Bianco et al., 2009) and has been observed to have increased activity during inflammation (Wong et al., 2000) and under membrane stress in red blood cells (Lopez et al., 2012). In accordance with these findings, increased activity was observed for acid sphingomyelinase RBC and plasma (Figure 3), as expected due to the membrane stress induced by RBC sickling. In further support of these findings, microparticles were observed to be elevated in SCD (Figure 7A-D), corroborating previous studies (Shet et al., 2003). In addition, microparticles were shown to have an increased ratio of ceramide to sphingomyelin (Figure 7G), which is indicative of acid sphingomyelinase activity through the hydrolysis of ceramide to produce sphingomyelin (Figure 2). SS microparticles were also characterized by significantly elevated S1P and sphingosine (Figure 7F). Dysregulation was observed for other enzymes and lipids in the sphingolipid metabolic pathway in SCD, including increased activity of ceramidase I in plasma (Figure 4B) and sphingosine kinase 2 (Figure 4C-4F) in RBC and plasma. S1P and sphingosine were both

observed to be elevated in whole blood (Figure 4G), plasma (Figure 4H), and RBCs (Figure 4I) in SCD.

Microparticle treatment increased the production and secretion of the inflammatory cytokines MIP-1α, IL-6, and TNF-α in macrophages (Figure 7). These specific cytokines have been associated with inflammation and vaso-occlusive crises in SCD (Keikhaei et al., 2013) and appear to induce an inflammatory phenotype in even non-inflammatory macrophages. IL-6 was constitutively produced and secreted in M0 and M2 macrophages in response to microparticle treatment, suggesting that microparticles may play a role in altering macrophage phenotype.

Additional studies elucidated sphingolipid dysregulation as a key factor initiating the activation of myeloid cells in SCD. Focus was placed on S1P as the most bioactive sphingolipid and the only sphingolipid with receptors. Recent studies have associated S1P with the recruitment of monocytes through the activity of S1P receptor 3 (Awojoodu et al., 2013; Keul et al., 2011). A physiological concentration of S1P increased monocyte adhesion to endothelial cells over four-fold (Figure 5), as did co-incubation with SS RBC (Figure 6). Together, these studies suggest that the elevation of S1P observed in RBCs, microparticles, and plasma in SCD may contribute to vaso-occlusion through RBC- or microparticle-mediated interactions and subsequent recruitment of these cells. Additional studies examining the direct effect of microparticles on myeloid cell adhesion will confirm these preliminary findings.

This pathway, through which RBC sickling initiates dysregulation of the sphingolipid metabolic pathway and contributes to vaso-occlusion, is a prime target for pharmacological treatment. Our results demonstrate that treatment with amitriptyline significantly reduced the generation of microparticles by RBCs *in vitro* and *in vivo* (Figure 8). Through the established connection between microparticles and myeloid cell activation, amitriptyline should impede

vaso-occlusion and inflammation by reducing microparticle generation and thus the recruitment, activation, and adhesion of myeloid cells. These results are promising, but additional studies are needed to directly relate the inhibition of acid sphingomyelinase to reduced recruitment of myeloid cells *in vivo* to confirm the effect of amitriptyline on myeloid cell recruitment and adhesion in SCD.

Currently, the primary treatment for sickle cell disease is blood transfusion, which replaces sickled red blood cells temporarily but does not influence the underlying causes of sickling (Health, 2002). The use of amitriptyline and other drugs to act on the sphingolipid metabolic pathway have shown to be dysregulated in sickle cell disease may prove to be a more effective treatment option. Pharmacological targeting of sphingolipids promise long-term treatment of the root causes of this devastating disease that is associated with chronic pain, stroke, organ failure, and low life expectancy (Belcher et al., 2000; Harmatz et al., 2000; National Institutes of Health, 2012) and that currently has no similar treatment options available.

REFERENCES

Aoki, S., Y. Yatomi, T. Shimosawa, H. Yamashita, J. Kitayama, N.H. Tsuno, K. Takahashi, and Y. Ozaki. 2007. The suppressive effect of sphingosine 1-phosphate on monocyte-endothelium adhesion may be mediated by the rearrangement of the endothelial integrins alpha(5)beta(1) and alpha(v)beta(3). *Journal Of Thrombosis And Haemostasis: JTH*. 5:1292-1301.

Awojoodu, A.O. unpublished.

Awojoodu, A.O., M.E. Ogle, L.S. Sefcik, D.T. Bowers, K. Martin, K.L. Brayman, K.R. Lynch, S.M. Peirce-Cottler, and E. Botchwey. 2013. Sphingosine 1-phosphate receptor 3 regulates recruitment of anti-inflammatory monocytes to microvessels during implant arteriogenesis. *Proceedings Of The National Academy Of Sciences Of The United States Of America*. 110:13785-13790.

Belcher, J.D., P.H. Marker, J.P. Weber, R.P. Hebbel, and G.M. Vercellotti. 2000. Activated monocytes in sickle cell disease: potential role in the activation of vascular endothelium and vaso-occlusion. *Blood*. 96:2451-2459.

Bianco, F., C. Perrotta, L. Novellino, M. Francolini, L. Riganti, E. Menna, L. Saglietti, E.H. Schuchman, R. Furlan, E. Clementi, M. Matteoli, and C. Verderio. 2009. Acid sphingomyelinase activity triggers microparticle release from glial cells. *The EMBO Journal*. 28:1043-1054.

Conran, N., C.F. Franco-Penteado, and F.F. Costa. 2009. Newer aspects of the pathophysiology of sickle cell disease vaso-occlusion. *Hemoglobin*. 33:1-16.

Cuvillier, O., G. Pirianov, B. Kleuser, P.G. Vanek, O.A. Coso, J.S. Gutkind, and S. Spiegel. 1996. Suppression of ceramide-mediated programmed cell death by sphingosine-1-phosphate. *Nature*. 381:800-803.

D'Alessandro, A., B. Blasi, G.M. D'Amici, C. Marrocco, and L. Zolla. 2013. Red blood cell subpopulations in freshly drawn blood: application of proteomics and metabolomics to a decades-long biological issue. *Blood Transfusion = Trasfusione Del Sangue*. 11:75-87.

Embury, S.H. 1986. The Clinical Pathophysiology of Sickle Cell Disease. *Annual Review of Medicine*. 37:361-376.

Gauley, J., and D.S. Pisetsky. 2010. The release of microparticles by RAW 264.7 macrophage cells stimulated with TLR ligands. *Journal of Leukocyte Biology*. 87:1115-1123.

Green, S.J., S. Mellouk, S.L. Hoffman, M.S. Meltzer, and C.A. Nacy. 1990. Cellular mechanisms of nonspecific immunity to intracellular infection: cytokine-induced synthesis of toxic nitrogen oxides from L-arginine by macrophages and hepatocytes. *Immunology Letters*. 25:15-19.

Gude, D.R., S.E. Alvarez, S.W. Paugh, P. Mitra, J. Yu, R. Griffiths, S.E. Barbour, S. Milstien, and S. Spiegel. 2008. Apoptosis induces expression of sphingosine kinase 1 to release sphingosine-1-phosphate as a "come-and-get-me" signal. *The FASEB Journal*. 22:2629-2638.

Hannun, Y.A., C. Luberto, and K.M. Argraves. 2001. Enzymes of Sphingolipid Metabolism: From Modular to Integrative Signaling. *Biochemistry*. 40:4893-4903.

Harmatz, P., E. Butensky, K. Quirolo, R. Williams, L. Ferrell, T. Moyer, D. Golden, L. Neumayr, and E. Vichinsky. 2000. Severity of iron overload in patients with sickle cell disease receiving chronic red blood cell transfusion therapy. *Blood*. 96:76-79.

Health, N.I.o. 2002. The management of sickle cell disease. *In* NIH Publication No. 02-2117, (4th ed.). National Institutes of Health, National Heart, Lung, Blood Institute, Division of Blood Diseases, Bethesda, MD.

Hebbel, R.P., O. Yamada, C.F. Moldow, H.S. Jacob, J.G. White, and J.W. Eaton. 1980. Abnormal adherence of sickle erythrocytes to cultured vascular endothelium: possible mechanism for microvascular occlusion in sickle cell disease. *The Journal Of Clinical Investigation*. 65:154-160.

Hughes, J.E., S. Srinivasan, K.R. Lynch, R.L. Proia, P. Ferdek, and C.C. Hedrick. 2008. Sphingosine-1-phosphate induces an antiinflammatory phenotype in macrophages. *Circulation Research*. 102:950-958.

Kaul, D.K., E. Finnegan, and G.A. Barabino. 2009. Sickle red cell-endothelium interactions. *Microcirculation (New York, N.Y.: 1994)*. 16:97-111.

Keikhaei, B., A.R. Mohseni, R. Norouzirad, M. Alinejadi, S. Ghanbari, F. Shiravi, and G. Solgi. 2013. Altered levels of pro-inflammatory cytokines in sickle cell disease patients during vaso-occlusive crises and the steady state condition. *European Cytokine Network*. 24:45-52.

Keul, P., S. Lucke, K. von Wnuck Lipinski, C. Bode, M. Gräler, G. Heusch, and B. Levkau. 2011. Sphingosine-1-phosphate receptor 3 promotes recruitment of monocyte/macrophages in inflammation and atherosclerosis. *Circulation Research*. 108:314-323.

Lopez, D.J., M. Egido-Gabas, I. Lopez-Montero, J.V. Busto, J. Casas, M. Garnier, F. Monroy, B. Larijani, F.M. Goni, and A. Alonso. 2012. Accumulated bending energy elicits neutral sphingomyelinase activity in human red blood cells. *Biophysical journal*. 102:2077-2085.

Madigan, C., and P. Malik. 2006. Pathophysiology and therapy for haemoglobinopathies. Part I: sickle cell disease. *Expert Reviews In Molecular Medicine*. 8:1-23.

Mause, S.F., and C. Weber. 2010. Microparticles: protagonists of a novel communication network for intercellular information exchange. *Circ Res*. 107:1047-1057.

Nathan, C. 1997. Inducible nitric oxide synthase: what difference does it make? *The Journal Of Clinical Investigation*. 100:2417-2423.

National Institutes of Health. 2012. What Is Sickle Cell Anemia? *In* Disease and Conditions Index. US Department of Health and Human Services, National Institutes of Health, National Heart, Lung, and Blood Institute.

Olivera, A., M.L. Allende, and R.L. Proia. 2013. Shaping the landscape: metabolic regulation of S1P gradients. *Biochimica Et Biophysica Acta*. 1831:193-202.

Peest, U., S.-C. Sensken, P. Andréani, P. Hänel, P.P. Van Veldhoven, and M.H. Gräler. 2008. S1P-lyase independent clearance of extracellular sphingosine 1-phosphate after dephosphorylation and cellular uptake. *Journal of Cellular Biochemistry*. 104:756-772.

Piccinini, M., F. Scandroglio, S. Prioni, B. Buccinnà, N. Loberto, M. Aureli, V. Chigorno, E. Lupino, G. DeMarco, A. Lomartire, M.T. Rinaudo, S. Sonnino, and A. Prinetti. 2010. Deregulated sphingolipid metabolism and membrane organization in neurodegenerative disorders. *Molecular Neurobiology*. 41:314-340.

Ratajczak, J., M. Wysoczynski, F. Hayek, A. Janowska-Wieczorek, and M.Z. Ratajczak. 2006. Membrane-derived microvesicles: important and underappreciated mediators of cell-to-cell communication. *Leukemia*. 20:1487-1495.

Shaner, R.L., J.C. Allegood, H. Park, E. Wang, S. Kelly, C.A. Haynes, M.C. Sullards, and A.H. Merrill, Jr. 2009. Quantitative analysis of sphingolipids for lipidomics using triple quadrupole and quadrupole linear ion trap mass spectrometers. *Journal Of Lipid Research*. 50:1692-1707.

Shet, A.S., O. Aras, K. Gupta, M.J. Hass, D.J. Rausch, N. Saba, L. Koopmeiners, N.S. Key, and R.P. Hebbel. 2003. Sickle blood contains tissue factor–positive microparticles derived from endothelial cells and monocytes. *Blood*. 102:2678-2683.

Tantawy, A.A., A.A. Adly, E.A. Ismail, N.M. Habeeb, and A. Farouk. 2012. Circulating platelet and erythrocyte microparticles in young children and adolescents with sickle cell disease: Relation to cardiovascular complications. *Platelets*.

van Meer, G., D.R. Voelker, and G.W. Feigenson. 2008. Membrane lipids: where they are and how they behave. *Nature Reviews. Molecular Cell Biology*. 9:112-124.

Wong, M.L., B. Xie, N. Beatini, P. Phu, S. Marathe, A. Johns, P.W. Gold, E. Hirsch, K.J. Williams, J. Licinio, and I. Tabas. 2000. Acute systemic inflammation up-regulates secretory sphingomyelinase in vivo: a possible link between inflammatory cytokines and atherogenesis. *Proc Natl Acad Sci U S A*. 97:8681-8686.